The development of the advanced cryogenic radiometer facility at NRC

Gamouras, A; Todd, A. D. W.; Côté, É; Rowell, N. L.

Publisher's version / Version de l'éditeur:
https://doi.org/10.1088/1742-6596/972/1/012014
Journal of Physics: Conference Series, 972, 2018-03-02

Journal of Physics: Conference Series

The development of the advanced cryogenic radiometer facility at NRC

IOP Conf. Series: Journal of Physics: Conf. Series **972** (2018) 012014 doi:10.1088/1742-6596/972/1/012014

The development of the advanced cryogenic radiometer facility at NRC

A Gamouras, A D W Todd, É Côté, and N L Rowell
National Research Council Canada, 1200 Montreal Road, Ottawa, Ontario, Canada
E-mail: angela.gamouras@nrc-cnrc.gc.ca

Abstract. The National Research Council (NRC) of Canada has established a next generation facility for the primary realization of optical radiant power. The main feature of this facility is a new cryogenic electrical substitution radiometer with a closed-cycle helium cryocooler. A monochromator-based approach allows for detector calibrations at any desired wavelength. A custom-designed motion apparatus includes two transfer standard radiometer mounting ports which has increased our measurement capability by allowing the calibration of two photodetectors in one measurement cycle. Measurement uncertainties have been improved through several upgrades, including newly designed and constructed transimpedance amplifiers for the transfer standard radiometers, and a higher power broadband light source. The most significant improvements in uncertainty arise from the enhanced characteristics of the new cryogenic radiometer including its higher cavity absorptance and reduced non-equivalence effects.

1. Introduction

Throughout the last few decades, the National Research Council (NRC) has continued to improve its primary scales in optical radiant power and spectral responsivity. Continuing with a detector-based realization, NRC transitioned from room-temperature electrical substitution absolute radiometers to a cryogenic absolute radiometer for most of the wavelength range in 1994 [1]. Now, two decades later, this cryogenic radiometer is at the end of its service life and is being replaced with an advanced radiometry facility equipped with a new, state-of-the-art cryogenic radiometer, broadband light sources and customized apparatus for increased measurement capability. Details of the new apparatus and the impact on the scale realization uncertainties from 300 nm to 1000 nm are presented.

2. Cryogenic radiometer apparatus

The configuration of NRC's new advanced radiometry facility is shown in Figure 1. The cryogenic radiometer (CryoRad III Radiometer: L-1 Standards and Technology, Inc.) is designed to accept optical radiation from the output of a monochromator illuminated with a broad-band light source. In this new facility, a laser-driven light source (LDLS) (EQ-99X: Energetiq Technology, Inc.) and a tungsten lamp were implemented to cover the spectral range of 250 nm to 2700 nm. These broad-band light sources were mounted on a linear translation stage at the monochromator entrance allowing for rapid and repeatable alignment to the monochromator entrance slit. Two concave spherical mirrors focused light from the output of a double-subtractive monochromator,

through a wavelength order sorting filter wheel to a tilted optical window mounted on a flexible vacuum bellows assembly. This large vacuum assembly was mounted on a linear stage with a pin and pivot system to rotate the cryogenic radiometer and transfer standard detectors for alignment to the common optical path (30° motion). The NRC transfer standard radiometers were designed and constructed with an integrated front window [1] which provided a vacuum seal when the radiometers were mounted to the evacuated vacuum bellows assembly. Isolation valves between the bellows vacuum chamber and the transfer radiometer mounting ports allowed the detectors to be changed during system operation. Fine adjustment of the transfer detector alignment was achieved using individual translation stages. To minimize the effect of any light source instabilities, transfer radiometer measurements were bracketed by cryogenic radiometer measurements. The radiant flux was also monitored using a separate detector that measures the reflection from the optical window.

To minimize any difference in the optical power incident to the cryogenic radiometer cavity and the transfer standard detectors, a circular aperture was mounted at the monochromator output resulting in a focused beam spot diameter of 5 mm. This spot diameter under-filled the cryogenic radiometer cavity input (7 mm diameter) as well as the input to the NRC transfer standard radiometers (6 mm diameter). The optical radiant power at the position of the cryogenic radiometer cavity varied with the selection of the light source and optical components in the system. In this case, two 600 groove/mm ruled diffraction gratings blazed at 500 nm were installed in the monochromator system. The LDLS yielded an optical radiant power at the cryogenic radiometer of 2.3 μW at 300 nm and 5.3 μW at 400 nm. When the tungsten lamp was aligned to the monochromator input, the optical radiant power at the cryogenic radiometer was 1.2 μW at 450 nm and 2.9 μW at 1000 nm.

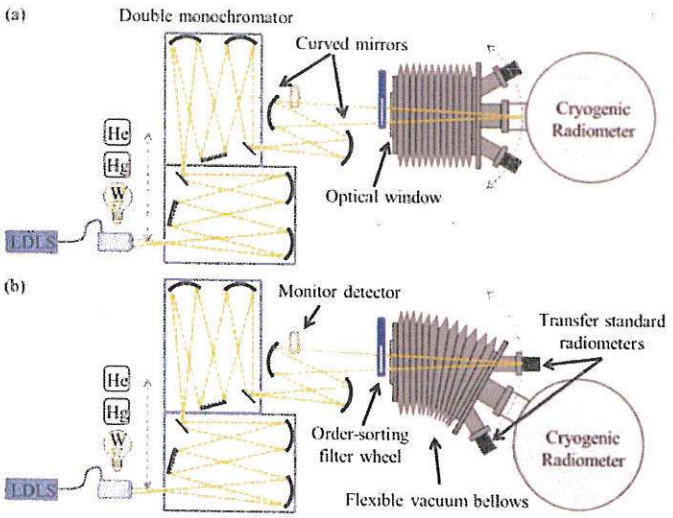

Figure 1. Schematic diagram of the optical power and spectral responsivity measurement apparatus. A motion platform aligns the output light from the monochromator with (a) the cryogenic radiometer or (b) a transfer standard detector. Helium and mercury light sources are used for monochromator wavelength calibration only.

In terms of functionality, this new facility has two main advantages over the previous measurement apparatus: the new cryogenic radiometer and the customized transfer standard mounting platform. The closed-cycle helium cryocooler incorporated into the cryogenic

radiometer design gives a greatly increased, uninterrupted run time when compared to traditional liquid helium cooled systems which require refilling of cryogens. The new apparatus has the option of mounting two transfer standard radiometers instead of one, with potential doubling of measurement capability per calibration cycle with the benefit of increased measurement redundancy.

3. Sources of uncertainty due to monochromator system

Primary optical power and spectral responsivity scales can be realized with different sources of optical radiation such as the use of multiple single line lasers and tunable laser sources [2–5]. Several combinations of monochromators and broadband light sources, including Argon arc plasma sources [6], Xe discharge lamps [7], and quartz-tungsten-halogen lamps [1, 8] have been implemented to span a wide spectral range in cryogenic radiometer measurements. When compared to laser-based primary realizations of optical radiant power, a monochromator-based approach offers the versatility of wavelength selection at the expense of laser line wavelength accuracy. As discussed below, some of the systematic differences between these methods arise due to the impact within our method of monochromator wavelength calibration, bandwidth effects, and stray light.

3.1. Wavelength calibration

For the present work, two 600 groove/mm ruled diffraction gratings blazed at 500 nm were installed in the double-subtractive monochromator system. Various spectral lines of helium and mercury lamps were used to calibrate the wavelength readout of each monochromator separately. The spectral lineshapes were fitted to a monochromator slit function, which for our case of a slit input and a round output is given by [9]:

$$I(\lambda) = \frac{1}{2} - \frac{2}{\pi}\left(\frac{2|\lambda-\lambda_0|}{\Delta} - 1\right)\left[\frac{|\lambda-\lambda_0|}{\Delta} - \frac{(\lambda-\lambda_0)^2}{\Delta^2}\right]^{\frac{1}{2}} - \frac{\sin^{-1}[(2|\lambda-\lambda_0|/\Delta) - 1]}{\pi} \quad (1)$$

where Δ is the monochromator bandwidth. Polynomial fits to the difference between published spectral line wavelengths and measured wavelengths were used to determine the wavelength correction curves for each of the two diffraction gratings. After the wavelength correction curves were applied to each monochromator, the residual wavelength uncertainty was found to be ± 0.05 nm. The magnitude of the corresponding uncertainties in responsivity were determined using the derivatives of the spectral responsivity curves for the transfer standard radiometers. Absolute rotary encoders mounted on the shaft of each motor are used to repeatably position the gratings (± 0.006 nm).

3.2. Monochromator bandwidth effects

The monochromator slit width was set to 1.0 mm, giving a bandpass of 4.4 nm. The effects of a finite bandwidth in this monochromator-based photodetector calibration system were evaluated and incorporated into the uncertainty budget using a similar approach to that described in Ref. [9]. In the case of a spectrally neutral reference detector, such as the cryogenic radiometer, bandwidth errors can be calculated using the measured spectral responsivity of a detector under test:

$$S_m^t(\lambda_0) = \frac{\int_{\lambda_0+\Delta}^{\lambda_0-\Delta} S^t(\lambda) I(\lambda) P(\lambda) d\lambda}{\int_{\lambda_0+\Delta}^{\lambda_0-\Delta} I(\lambda) P(\lambda) d\lambda} \quad (2)$$

where S^t and S_m^t are the true and measured spectral responsivity of the detector under test, $P(\lambda)$ is the spectral distribution of the monochromator output, and $I(\lambda)$ is the monochromator

slit function given in Equation 1. The relative bandwidth error is given by:

$$\epsilon(\lambda_0) = \frac{[S_m^t(\lambda_0) - S^t(\lambda_0)]}{S^t(\lambda_0)}. \tag{3}$$

The unknown quantity S^t is required to solve Equations 2 and 3. A cubic spline interpolation of the measured spectral responsivity data was used in place of S^t, and the corresponding calculated uncertainties due to bandwidth effects from 300 nm to 1000 nm are shown in Table 1.

3.3. Monochromator stray light

Out of band stray light can be caused by scattering, diffraction, or multiple reflections from inside the monochromator. Although stray light levels are usually considered negligible for double monochromators, we decided to test this assumption for the new apparatus. The photocurrent of a single-element silicon transfer standard radiometer was measured from 250 nm to 700 nm with and without an RG665 long pass filter in the beam (Fig. 2). The stray light component of the signal was found to be relatively insignificant: <0.01 % for the LDLS above 300 nm and <0.01 % for the tungsten lamp above 400 nm. The tungsten lamp was only used for spectral responsivity measurements above 400 nm. As the cryogenic radiometer cavity and transfer standard radiometers are coplanar and have similar sized input aperture diameters, the effect of stray light was considered to be negligible.

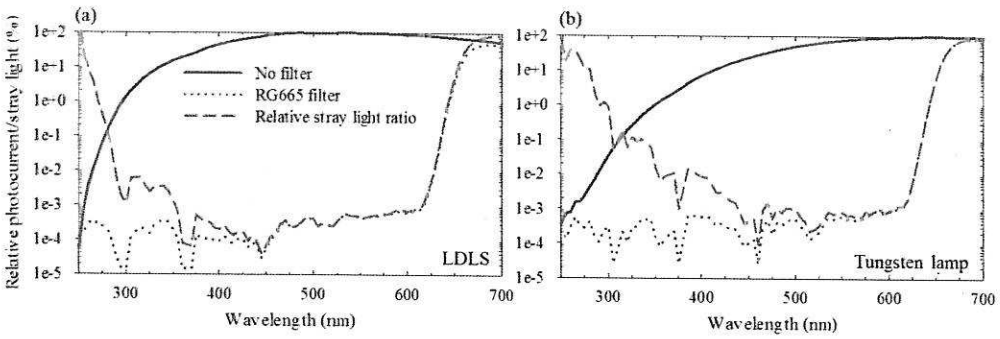

Figure 2. Measured stray light levels in the double monochromator system with (a) the LDLS and (b) the tungsten lamp. A 280 nm long pass filter was mounted to the LDLS output for all measurements to minimize exposure of optical components to UV radiation.

4. Measurement uncertainties

NRC's new absolute radiometry facility has demonstrated significant improvements to its realization of the optical power scale. A complete uncertainty budget for calibrations of single-element silicon transfer standard radiometers using a monochromator and broad-band light source includes wavelength calibration, bandwidth, and temperature effects. These spectrally-dependent uncertainties for spectral responsivity calibrations are listed in Table 1. The repeatability component was estimated by taking the standard deviation of eight measurement cycles. The non-uniformity of the transfer standard detectors has been previously characterized [1] and is accounted for indirectly by the measurement repeatability. The transfer radiometer photocurrent measurement uncertainty component was estimated from the specifications for

the digital multimeter (Agilent Technologies 3458A Multimeter) and from the characterization of the NRC-built transimpedance amplifiers used to convert the transfer standard detector photocurrent to a voltage signal.

Table 1. Uncertainty budget for monochromator-based calibrations of single-element silicon transfer standard radiometers (%).

Source of Uncertainty / Wavelength (nm)	Cryogenic Radiometer Effects	Transfer Radiometer Photocurrent Measurement	Measurement Repeatability	Mono. Wavelength Calibration (± 0.05 nm)	Mono. Bandwidth Effects	Transfer Radiometer Temperature (± 0.5°C)	Overall Uncertainty (%)
300	0.011	0.004	0.019	0.013	0.0094	0.008	0.028
320	0.011	0.004	0.008	0.011	0.0096	0.003	0.021
340	0.011	0.004	0.007	0.002	0.0249	0.001	0.029
360	0.011	0.004	0.004	0.003	0.0354	0.016	0.041
380	0.011	0.004	0.006	0.020	0.0180	0.015	0.034
400	0.011	0.004	0.004	0.019	0.0093	0.014	0.028
450	0.011	0.004	0.004	0.009	0.0002	0.009	0.018
500	0.011	0.004	0.004	0.007	0.0006	0.006	0.016
550	0.011	0.004	0.005	0.006	0.0001	0.004	0.015
600	0.011	0.004	0.007	0.005	0.0001	0.004	0.015
650	0.011	0.004	0.007	0.005	0.0000	0.004	0.015
700	0.011	0.004	0.006	0.004	0.0000	0.003	0.014
750	0.011	0.004	0.011	0.004	0.0000	0.004	0.017
800	0.011	0.004	0.014	0.004	0.0000	0.002	0.019
850	0.011	0.004	0.018	0.003	0.0002	0.001	0.022
900	0.011	0.004	0.008	0.004	0.0005	0.002	0.015
950	0.011	0.004	0.010	0.001	0.0027	0.009	0.018
1000	0.011	0.004	0.010	0.006	0.0061	0.128	0.129

Table 2 summarizes the changes in the uncertainty budget between NRC's previous and new absolute cryogenic radiometers. Contributions due to cavity absorptance and non-equivalence effects have had the most significant impact.

Table 2. Uncertainties due to cryogenic radiometer (k=1).

Source of Uncertainty	Magnitude-Old [10] (%)	Magnitude-New (%) [11]
Cryogenic radiometer cavity absorptance	0.01	0.001
Cryogenic radiometer electrical-power measurement	0.01	0.011
Cryogenic radiometer nonequivalence effects	0.01	0.002
Overall Cryogenic Radiometer Effects	0.017	0.011

5. Conclusions

NRC has a new state-of-the-art facility for the primary realization of optical radiant power. A new absolute cryogenic radiometer provides for significant improvements in uncertainty for the realization of the optical power scale, significantly reducing the overall cryogenic radiometer uncertainty contribution from the 0.017 % to 0.011 %. A wavelength dependent uncertainty budget from 300 nm to 1000 nm for silicon detector calibrations was presented. Future work will include the extension of calibration capabilities into the ultraviolet and infrared wavelength ranges with appropriate monochromator diffraction gratings and optical window for the vacuum bellows system.

6. Acknowledgments

The authors would like to acknowledge Jason Demers and the team at NRC Design and Fabrication Services for their contributions to the design, manufacture, and assembly of the motion platform system, transfer detector mounts, and vacuum bellows components.

7. Disclaimer

The commercial equipment identified in this paper are for informative purposes only. Such identification does not imply recommendation or endorsement by NRC, nor does it imply that the equipment is necessarily the best available for the purpose.

References

[1] Boivin L P and Gibb K 1995 *Metrologia* **32** 565
[2] Gentile T R, Houston J M, Hardis J E, Cromer C L and Parr A C 1996 *Appl. Opt.* **35** 1056–1068
[3] Werner L, Fischer J, Johannsen U and Hartmann J 2000 *Metrologia* **37** 279
[4] Eppeldauer G P, Larason T C, Houston J M, Vest R E, Arp U and Yoon H W 2014 *Metrologia* **51** S252
[5] Hong K S, Park S, Kim S K, Park S N and Lee D H 2015 *Journal of the Korean Physical Society* **67** 2045–2058
[6] Meindl P, Klinkmüller A E, Werner L, Johannsen U and Grützmacher K 2006 *Metrologia* **43** S72
[7] Corróns A, Fontecha J L, Corredera P, Campos J, Pons A and Hernanz M L 2000 *Metrologia* **37** 555
[8] Schrama C A, Bosma R, Gibb K, Reijn H and Bloembergen P 1998 *Metrologia* **35** 431
[9] Boivin L P 2002 *Appl. Opt.* **41** 1929–1935
[10] Boivin L P 1998 *Metrologia* **35** 363
[11] L-1 Standards and Technology, Inc 2015 Cryorad-III characterization results